Int J Appl Earth Obs Geoinformation 73 (2018) 420–427

Contents lists available at ScienceDirect

Int J Appl Earth Obs Geoinformation

journal homepage: www.elsevier.com/locate/jag

Linking Landsat to terrestrial LiDAR: Vegetation metrics of forest greenness are correlated with canopy structural complexity

Elizabeth A. LaRue[a,*], Jeff W. Atkins[b], Kyla Dahlin[c], Robert Fahey[d], Songlin Fei[a], Chris Gough[b], Brady S. Hardiman[a,e]

[a] Dept. of Forestry & Natural Resources, Purdue University, 715 W. State Street, West Lafayette, IN, 47907, United States
[b] Dept. of Biology, Virginia Commonwealth University, 1000 W. Cary Street, Richmond, VA, 23284, United States
[c] Dept. of Geography, Environment, and Spatial Sciences and Program in Ecology, Evolutionary Biology, and Behavior, Michigan State University, 673 Auditorium Rd., East Lansing, MI, 48824, United States
[d] Dept. of Natural Resources and the Environment and Center for Environmental Sciences and Engineering, University of Connecticut, 1376 Storrs Road, Storrs, CT, 06269, United States
[e] Dept. of Ecological and Environmental Engineering, Purdue University, 715 W. State Street, West Lafayette, IN, 47907, United States

ARTICLE INFO

Keywords:
Eastern North American forests
Canopy structure
Portable canopy LiDAR
NDVI
NEON
Terrestrial LiDAR

ABSTRACT

Vegetation metrics derived from satellite imagery provide continuous and large spatial-scale measurements that are critical for interpreting and predicting ecosystem function. However, uncertainty still remains as to the precise structural information that could be estimated from these metrics. Landsat-derived metrics provide pixel measurements of vegetation across the landscape, whereas Light Detection and Ranging (LiDAR) provides multidimensional data on the vertical arrangement of forests. Terrestrial LiDAR metrics of structural complexity describe the arrangement of vegetation in the canopy, and could be coupled with Landsat-derived metrics through their influence on energy and light. Linking Landsat to terrestrial LiDAR estimates of canopy structure could expand the interpretation of Landsat-derived metrics and broaden the spatial scale at which structural complexity can be evaluated. Here, we examined associations between Landsat-derived metrics and terrestrial LiDAR measurements of structural complexity. Structural complexity measurements were obtained with terrestrial LiDAR from plots within eight forested NEON sites across eastern North America. Vegetation metrics (NDVI, EVI, tasseled cap metrics) were calculated for corresponding locations from Landsat 8 satellite imagery. Results showed that canopy reflectance, greenness and brightness, were linked with several measures of canopy structure. Higher levels of greenness were associated with stands having a taller canopy, greater leaf area density and variability, and a less open and porous canopy. Among greenness metrics, NDVI was most strongly correlated with structural complexity metrics (adj. R^2 = 0.52 – 0.62 for six metrics). Additionally, we found that a brighter canopy was associated with greater leaf area density and variability, canopy cover, porosity, and lower leaf clumping. Our results demonstrated the potential for large-spatial extent estimates of structural complexity using satellite imagery, and may lead to improved predictions of forest ecosystem functioning such as those predicted in "big leaf" ecosystem models.

1. Introduction

Vegetation metrics have long been inferred from satellite imagery (Crist and Cicone, 1984), but understanding the structural information represented in these spectrally-derived proxies remains challenging (Huete et al., 2002). Vegetation metrics modeled from global Landsat imagery include information on canopy greenness (Gamon et al., 1995; Huete et al., 2002), brightness, and water content (Crist and Cicone, 1984). The metrics of greenness, NDVI and EVI, are widely used as proxies for leaf area and vegetation cover (Zheng and Moskal, 2009). These continuous and large spatial-scale measurements are critical for interpreting and predicting ecosystem function at landscape to global scales (Glenn et al., 2008; Fisher et al., 2018). However, uncertainty remains in understanding which structural information can be represented by Landsat-derived metrics (e.g. Huete et al., 2002).

Satellite imagery and terrestrial Light Detection and Ranging (LiDAR) are typically applied to characterize different features of vegetation, but may provide related information on multidimensional

* Corresponding author.
E-mail address: elarue@purdue.edu (E.A. LaRue).

https://doi.org/10.1016/j.jag.2018.07.001
Received 24 April 2018; Received in revised form 12 June 2018; Accepted 2 July 2018
Available online 18 July 2018
0303-2434/

structure. LiDAR creates detailed three-dimensional profiles of forest structure (Nychka and Nadkarni, 1990). Specifically, terrestrial LiDAR is useful for measuring different aspects of canopy structural complexity (hereafter structural complexity), which is the *arrangement* (rather than *quantity*) of leaf area within the canopy (Parker et al., 2004; Hardiman et al., 2011, 2013a). The structural complexity of forest canopies provides a linkage to mechanistically predict how forest structure influences ecosystem function (Hardiman et al., 2011, 2013a; Fahey et al., 2015). Previous studies that have used optical satellite imagery to map forest structure in comparison to LiDAR have primarily focused on tree height or biomass (Matasci et al., 2018), but none have focused on the potential to use Landsat-derived metrics as proxies of canopy structural complexity. Linking common Landsat-derived metrics to structural complexity metrics from terrestrial LiDAR could broaden understanding of the structural information represented by vegetation metrics. Furthermore, large spatial-scale prediction of structural complexity could improve the prediction of biogeochemical cycling and ecosystem functioning using "big leaf" ecosystem models (Fisher et al., 2018).

Canopy greenness and brightness derived from Landsat may contain more information than previously expected about structural complexity, with the two coupled through their shared relationship with canopy light distribution and interception (Funk and Lerdau, 2004). Landsat-derived metrics could therefore be correlated with metrics of structural complexity (Table 1). Structural complexity as measured by terrestrial LiDAR can be grouped into categories that describe how vegetation is distributed within the canopy: canopy height, density and area, arrangement, cover, and variability (Atkins et al., 2018b, In Review). Taller (Freitas et al., 2005), more heterogeneous (Hardiman et al., 2011), dense (Ren et al., 2015), and clumped canopies (Thomas et al., 2011) might also be greener and more reflective (Table 1) (Gemmell, 1995; Freitas et al., 2005), because these structural complexity metrics are also correlated with light acquisition (Atkins et al., 2018a) and higher forest productivity (Hardiman et al., 2011; 2013b, Fahey et al., 2016). In contrast, heterogeneous or less dense canopies may be darker (Baldocchi and Harvey, 1995; Law et al., 2001), because rougher canopies scatter a greater fraction of incident light (Ogunjemiyo et al., 2005; Atkins et al., 2018a). A correlation between wetness and all five categories of structural complexity across sites and forest types is likely to be negligible, because structure across forest types may not have a strong mechanistic link to canopy water content.

Terrestrial LiDAR provides detailed measurements of structural complexity at a sub-hectare spatial scale (Parker et al., 2004; Hardiman et al., 2013b), but covering areas larger than this can be logistically challenging. The prohibitive cost and time requirements have limited the quantification of structural complexity in ecological studies at larger spatial extents, but Landsat imagery is globally available (Glenn et al., 2008). The ability to link structural complexity with Landsat-derived metrics could provide the potential to understand multi-dimensional forest structure at a larger spatial extent and could even improve global predictions of ecosystem function. Our overall objective was to evaluate relationships between Landsat-derived metrics of vegetation and terrestrial LiDAR metrics of structural complexity within forest canopies of Eastern North America (Table 1).

2. Methods

2.1. Study sites

We evaluated relationships between Landsat-derived vegetation metrics and LiDAR-derived metrics of structural complexity across eight National Ecological Observatory Network (NEON) sites (Fig. 1A) spanning six ecoclimatic domains of eastern North America (Appendix 1: Table S1). Within each site, we collected terrestrial LiDAR and Landsat imagery from $N = 5$–20 plots (40 x 40 m) (Kao et al., 2012). NEON site information and design can be found at http://www.neonscience.org/science-design/field-sites/list.

2.2. Structural complexity metrics from terrestrial LiDAR

We used a terrestrial portable canopy LiDAR system based on the design by Parker et al. (2004) to collect structural complexity from within NEON plots. Briefly, high frequency laser pulses are emitted from the LiDAR unit and reflect off canopy surfaces as an operator moves the unit along a transect at a constant speed. Both reflected and un-reflected pulses are used to reconstruct a representative vertical cross section through the canopy, illustrating the spatial configuration of surface area within the canopy volume. From this cross-section, structural complexity is characterized via a suite of structural metrics describing 2D and 3D heterogeneity of foliage. Structural metrics describing the arrangement of leaf area are related to, but not identical to, the amount of leaf area in the canopy (Appendix 2). For details on the design, calibration, operation, and validation of the portable canopy LiDAR system see Parker et al. (2004).

Metrics of structural complexity that we measured by terrestrial

Table 1
Predictions for how Landsat-derived metrics might be correlated with LiDAR structural complexity metrics.

Structural complexity	Description	Predicted positive (+) or negative (−) correlation with mean of Landsat-derived metrics		
		Canopy greenness (NDVI, EVI, TC Greenness)	TC Brightness	TC Wetness
Height				
Mean leaf height	Transect mean of column mean leaf height – mean of density-adjusted vegetation heights per each column	+	+	negligible
Mean outer canopy height	Mean of the column maximum canopy height	+	+	negligible
Area and density				
Mean height of VAI_{Max}	Mean height of VAI_{Max} across a transect	+	+	negligible
Mean VAI	Mean of column summed vegetation area index	+	+	negligible
Cover				
Cover fraction	Transect mean of column ratio of canopy hits relative to total leaf returns	+	+	negligible
Heterogeneity				
Mean of vertical SD	Transect mean of column variability of mean leaf height	+	–	negligible
Rugosity	Transect variability of column variability of leaf density	+	–	negligible
Top rugosity	Transect variability of column maximum canopy height	+	–	negligible
Arrangement				
Porosity	Ratio of bins with no leaf area to total bins	–	+	negligible
Clumping metric	Degree of foliar clumping	+	–	negligible

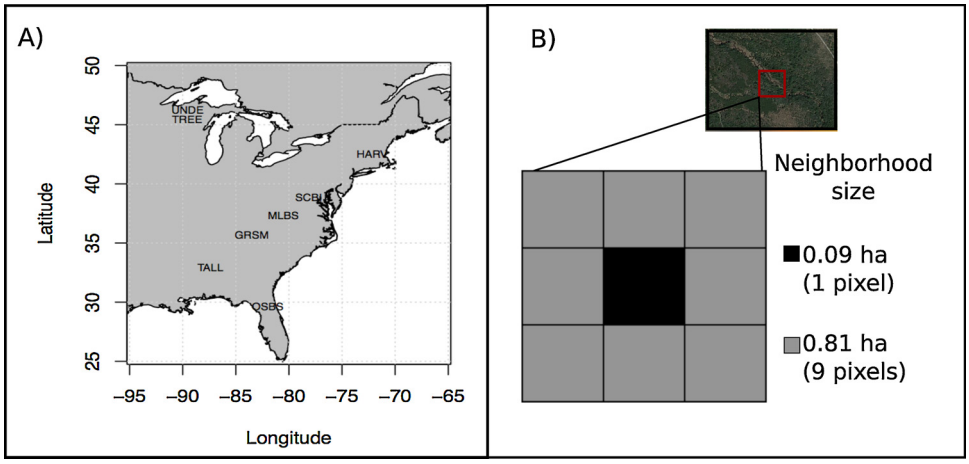

Fig. 1. Sampling sites and plots. A) NEON sampling site locations. B) Neighborhood size of Landsat-derived metrics at sampled 40 x 40 m NEON base plots. The 40 x 40 m NEON base plot overlapped with the center 30 x 30 m Landsat pixel.

LiDAR can be grouped into five categories (Table 1; Parker et al., 2004; Hardiman et al., 2011; Atkins et al., 2018b, In Review). These include 1) height metrics that describe the distribution of tree and leaf heights within the canopy; 2) density metrics that describe the volume, area, and density of leaves within the canopy; 3) arrangement metrics that describe the 3D distribution of vegetation architecture within the canopy; 4) cover and openness metrics; and 5) variability metrics that describe 3D leaf arrangement and variability (Hardiman et al., 2013b; Atkins et al., In Review). We calculated 10 metrics that fall within these five categories of structural complexity that are defined in Table 1 (Hardiman et al., 2013b; Atkins et al., 2018b, In Review). We measured structural complexity from terrestrial portable canopy LiDAR data collected along two to three 40 m transects within each plot during the 2016 growing season (further described in Atkins et al., 2018a). The raw data from each transect was processed with the *forestr* package in R (Atkins et al., 2018b, In review) to produce 10 structural complexity metrics. We calculated the plot-level mean (means of transects collected within each plot) and the site-level mean (the mean of all plots within each site) of structural complexity metrics. Additional details on the definition, derivation, and calculation of these metrics are available in Atkins et al. (In Review; forestr package in R).

2.3. Landsat-derived metrics

We downloaded Landsat 8 Pre-Collection top of atmosphere and surface reflectance imagery from the USGS Earth Explorer (usgs.earthexplorer.gov) for each of the eight NEON sites to derive vegetation metrics. We selected one cloud-free image from the 2016 growing season, but if multiple suitable images were available then we used imagery with the closest acquisition date to that of the portable canopy LiDAR data. Landsat imagery was extracted from each NEON location and all image digital numbers were converted to top of atmosphere and surface reflectance values using coefficients provided in scene metadata. We extracted band data at two neighborhood sizes to account for the potential of imperfect overlap of pixel and plot sizes, because the NEON plot size is larger than the Landsat image pixels. The first neighborhood size was a single 30 x 30 m pixel (900 m^2, 0.09 ha) at the center of each 40 x 40 m NEON base plot (1600 m^2, 0.16 ha) (Fig. 1B). We also extracted band data from a 9-pixel neighborhood (3 × 3; 0.81 ha) centered on each plot (i.e. we took the adjacent 8 pixels in addition to the center pixel). Five metrics were then calculated for each pixel, including the normalized difference vegetation metric, (NDVI; Tucker, 1979), enhanced vegetation metric (EVI, Huete et al., 2002), and the tasseled cap brightness, greenness, and wetness transformations (Crist and Cicone, 1984; Baig et al., 2014). These five metrics were chosen because they represent some of the most widely used Landsat vegetation indices as our study was not meant to be an exhaustive exploration of all possible correlations between canopy structural complexity and spectral data. The plot-level average and standard deviation of metric values were calculated across the 9-pixel neighborhood size. The site-level means (average of plots within sites) of Landsat-derived metrics were also calculated. Landsat data was extracted and processed in R 3.4.1 (The R Group).

2.4. Statistical analyses

Prior to conducting statistical analyses, sampled plots were arbitrarily assigned to either a model calibration (80%) or validation (20%) dataset (N_{Plots} = 69, 17, respectively). Several variables were first ln (x + 1) transformed to meet model assumptions, including: mean NDVI, EVI, tasseled cap (TC) brightness and wetness; the standard deviation of NDVI, EVI, and TC brightness; mean outer canopy height, mean VAI, mean of vertical SD, rugosity, and the cover fraction. All analyses were conducted in R 3.4.1.

Before we tested our study objectives, we evaluated whether or not there was a difference in the strength of the relationship between Landsat-derived and structural complexity metrics at the 1- or 9-pixel neighborhood size. This step was necessary to determine if resolution differences between Landsat pixels and the area of NEON plots would affect analysis results. Furthermore, relationships were significant following log-transformation, therefore we tested for linear terms in our analyses. A detailed description of analyses and results for this step can be found in Appendix 3; briefly, the 1-pixel for NDVI and EVI and 9-pixel for the tasseled cap transformations were chosen to be used for all analyses.

2.4.1. Analyses between plot-level Landsat-derived and structural complexity metrics

We used linear regressions to test relationships among Landsat-derived metrics and LiDAR structural complexity metrics across all plots (N_{Plots} = 69). First, we tested for significant relationships between plot-level means of Landsat-derived and structural complexity metrics with univariate linear regressions; a Landsat-derived metric was the predictor and a structural complexity metric the response variable in each analysis. Next, we tested for significant correlations between the standard deviation (in the 9-pixel neighborhood) of Landsat-derived and structural complexity metrics. Correlation coefficients between structural complexity metrics may also be found in Appendix 3: Table S2. Finally, we also tested for the potential of the leaf area index to explain much of the variation between Landsat-derived metrics and structural

complexity; the methods and results for this analysis are presented in Appendix 2.

We also used multivariate regression to explore if multiple Landsat-derived predictors would have greater potential to explain variation in structural complexity metrics at the plot-level. We constructed models of Landsat-derived metrics that predict variation within each structural complexity metric with stepwise multiple regression and AIC using the MASS package in R (Venables and Ripley, 2002). We removed EVI from multiple regression analyses, because it was highly correlated with NDVI ($|R| = 0.92 >$ our threshold level of an $|R| > 0.70$ to avoid collinearity; Dormann et al., 2013). A stepwise regression with AIC was then conducted for Landsat-derived metrics as predictor variables and for each of the 10 structural complexity metrics as separate response variables.

2.4.2. Analyses between site-level Landsat-derived and structural complexity metrics

We tested for significant linear relationships between Landsat-derived and structural complexity metrics at the site-level with randomization tests ($N_{Sites} = 8$). The mean of structural complexity metrics and Landsat-derived metrics at each site violated the assumption of normality, so we used a non-parametric randomization test (Pitman, 1938). A probability distribution based on the existing dataset is used in a randomization test to assess the significance of a test-statistic in linear regression without violating model assumptions (Pitman, 1938). Therefore, we assessed the significance of the overall model F-statistic between the site means of Landsat-derived metrics and structural complexity metrics with a randomization test. The adjusted R^2 was considered significant if the actual F-statistic was greater than 0.05 of the proportion of 9999 randomly generated F-statistics from the observed data.

2.4.3. Prediction of structural complexity metrics

To identify candidate structural complexity metrics that can be robustly estimated from Landsat-derived metrics, we tested the reliability of predictions made by univariate and multiple regression models that had an overall model R^2 greater than 0.5. Landsat-derived metrics from the randomly-selected 20% validation dataset ($N_{plots} = 17$) was used to test the ability of univariate and multiple regression models from section 2.4.1 to predict new values of structural complexity as compared to their actual observed values. We took the difference between predicted and observed structural complexity values and estimated the distribution of the mean difference with bootstrapping. The accelerated 95% confidence interval of each generated distribution (Efron and Tibshirani, 1986) was compared to an expected value of zero to determine whether regression models over or under-predicted new structural complexity values.

3. Results

3.1. Plot- and site-level correlations between Landsat-derived and structural complexity metrics

We found that Landsat-derived metrics of greenness were correlated with multiple structural complexity metrics. Canopy greenness increased with height, leaf area density, cover, and variability at the plot-level, while canopy greenness decreased with metrics describing canopy arrangement (Table 2). NDVI, EVI, and TC greenness were significantly related to nine, eight, and seven of the ten structural complexity metrics, respectively (Table 2). The sign of these relationships was positive for all three Landsat metrics of greenness, except for TC greenness, which was negatively correlated with porosity. Of three metrics that measure canopy greenness, NDVI was most strongly related to structural complexity metrics (Table 2), with an adjusted R^2 greater than 0.5 for six metrics (Fig. 2). Conversely, EVI and TC greenness were not as strongly correlated with structural complexity metrics (adjusted $R^2 = 0.46, 0.23$, respectively; Table 2).

TC brightness was positively correlated with leaf area density, canopy cover, canopy variability and arrangement across NEON plots, whereas TC wetness was not correlated with any structural complexity metrics (Table 2). Lower values of TC brightness were associated with larger values of canopy rugosity and the clumping metric (Table 2). TC brightness exhibited the strongest relationships with categories of leaf density, cover, and arrangement, but none of the significant correlations between TC brightness and any of the structural complexity metrics were especially strong (adjusted $R^2 = 0.07–0.32$). Conversely, TC wetness was not significantly correlated with any of the canopy structural complexity metrics at the plot-level (Table 2).

We found that the variation in Landsat-derived metrics across the 9-pixel neighborhood was significantly associated with several structural complexity metrics at the plot-level (Table 3). The direction of the relationship between standard deviation of Landsat-derived metrics across the 9-pixel neighborhood and structural complexity varied depending on the individual metric (Table 3). The strongest relationship was observed between the standard deviation of TC brightness within plots and seven structural complexity metrics ($R^2 = 0.11–0.37$). We found that the standard deviation of NDVI within plots was associated with five metrics ($R^2 = 0.09–0.13$), EVI with three metrics ($R^2 = 0.10–0.12$), and TC greenness with one metric of structural complexity ($R^2 = 0.11$).

Positive site-level relationships (mean of plots within a site) occurred between three Landsat-derived and structural complexity metrics. NDVI was significantly associated with three structural complexity metrics, including Ln(mean VAI), Ln(cover fraction), and porosity ($R^2 = 0.66, 0.67, 0.56$, respectively; $p < 0.05$). NDVI was marginally significantly associated with Ln(mean of vertical SD) and Ln (rugosity) ($R^2 = 0.48, 0.44$, respectively; $p < 0.10$). We also observed that Ln(mean VAI), Ln(cover fraction), and porosity were significantly positively correlated with EVI ($R^2 = 0.42, 0.43, 0.44$, respectively). One metric, clumping index ($R^2 = 0.38$), was marginally negatively ($p < 0.10$) associated with TC brightness. There were no significant relationships between TC greenness and wetness with structural complexity metrics. Overall, there were fewer significant correlations between Landsat-derived metrics and structural complexity at the site-level than plot-level analyses.

3.2. Estimation of structural complexity metrics with NDVI

We chose six multiple regression and six univariate models with adjusted $R^2 > 0.5$ (Appendix 3: Table S3, 4, respectively) to evaluate model estimates of six structural complexity metrics against a validation dataset. Overall, Landsat-derived metrics in multiple regression and univariate NDVI models, robustly predicted five and six of the chosen six structural complexity metrics, respectively, in the model validation dataset (Fig. 3). Specifically, we found that the 95% confidence intervals of the bootstrapped mean difference between predicted and observed structural complexity values (20% validation dataset, $N_{Plots} = 17$) from multiple regression overlapped with zero for five of the six structural complexity metrics (i.e. the model did not over or under predict), excluding rugosity (Fig. 3A). The 95% confidence intervals of the bootstrapped mean difference between predicted and observed structural complexity values from simple linear regression with NDVI overlapped with zero for all six metrics (Fig. 3B).

4. Discussion

Our study shows that two-dimensional vegetation metrics contain signatures of three-dimensional canopy structure. We found that Landsat vegetation indices from across eastern North America were correlated with multiple structural complexity measures from terrestrial LiDAR. Landsat-derived metrics of canopy greenness and brightness explained 7% to 62% of variation in five categories of structural

Table 2
Adjusted R^2 (correlation coefficients) of univariate linear regressions between Landsat-derived metrics and structural complexity metrics. An adjusted R^2 that was significantly different from zero at $\alpha < 0.05$ is shown, while those that were non-significant are depicted as NS.

	Parameters	Ln(NDVI) (1-pixel)	Ln(EVI) (1-pixel)	TC Greenness (9-pixel)	Ln(TC Brightness) (9-pixel)	Ln(TC Wetness) (9-pixel)
Height	Mean leaf height	0.21 (14.97)	0.16 (24.61)	NS	NS	NS
	Ln(mean outer canopy height)	0.55 (3.59)	0.40 (5.73)	0.17 (0.62)	NS	NS
Area and density	Mean height of VAI_{Max}	0.12 (11.13)	0.09 (17.82)	NS	NS	NS
	Ln(mean VAI)	0.62 (3.68)	0.46 (5.89)	0.23 (5.97)	0.21 (6.45)	NS
Cover	Ln(cover fraction)	0.58 (3.73)	0.41 (5.90)	0.21 (12.16)	0.17 (9.80)	NS
Heterogeneity	Ln(mean of vertical SD)	0.56 (7.94)	0.42 (12.79)	0.19 (12.43)	0.09 (8.60)	NS
	Ln(rugosity)	0.52 (7.15)	0.37 (11.31)	0.23 (8.08)	0.07 (−8.61)	NS
	Top rugosity	NS	NS	NS	NS	NS
Arrangement	Porosity	0.53 (−0.67)	0.38 (−1.06)	0.12 (5.99)	0.32 (6.18)	NS
	Clumping metric	0.14 (−0.24)	0.04 (−0.26)	0.06 (−0.43)	0.15 (−0.72)	NS

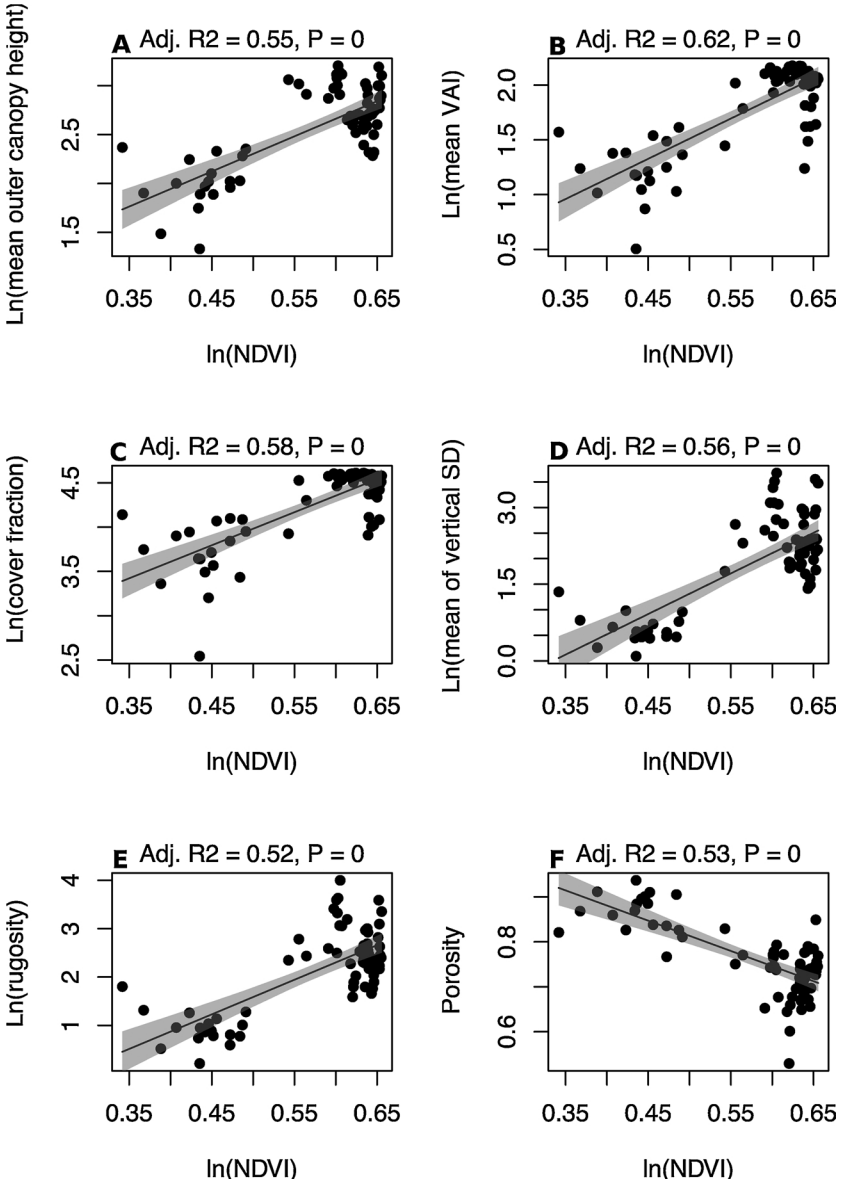

Fig. 2. NDVI explains variation in several structural complexity metrics across plots in eight forested sites within the Eastern US. A) The mean outer canopy height, B) mean VAI, C) the canopy cover fraction, D) the mean vertical standard deviation of leaf height, E) rugosity, F) porosity. The adjusted R^2 for the regression between Ln (NDVI) and each canopy structural complexity metric shown was greater than 0.50 for a calibration dataset composed of 80% of the total dataset. The line of best fit and 95% confidence intervals are shown.

Table 3
Adjusted R^2 (correlation coefficients) of univariate linear regressions between the standard deviation of Landsat-derived metrics within a 9-pixel neighborhood and structural complexity metrics. An adjusted R^2 that was non-significant is show as NS.

	Parameter	Ln(NDVI)	Ln(EVI)	Ln(TC Brightness)	TC Greenness	TC Wetness
Canopy height	Mean leaf height	NS	NS	NS	NS	NS
	Ln(mean outer canopy height)	NS	NS	0.23 (−4.66)	NS	NS
Leaf area density	Mean height of VAI_{Max}	NS	NS	NS	NS	NS
	Ln(mean VAI)	0.12 (−8.89)	0.10 (20.87)	0.37 (−5.70)	NS	NS
Canopy cover	Ln(cover fraction)	0.09 (−8.32)	0.10 (22.13)	0.34 (−5.70)	NS	NS
Canopy variability	Ln(mean of vertical SD)	0.12 (−19.96)	NS	0.30 (−11.61)	NS	NS
	Ln(rugosity)	0.09 (−16.82)	NS	0.32 (−11.28)	NS	NS
	Top rugosity	NS	NS	NS	NS	NS
Canopy arrangement	Porosity	0.13 (1.84)	NS	0.29 (1.00)	0.11 (1.54)	NS
	Clumping metric	NS	0.12 (−3.00)	0.11 (0.42)	NS	NS

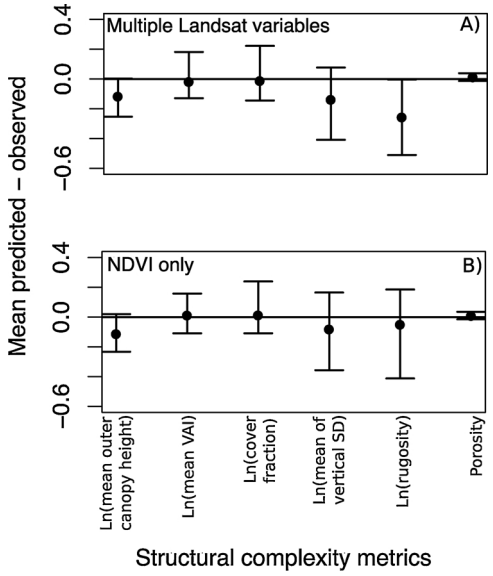

Fig. 3. Bootstrapped mean difference between observed and predicted structural complexity values from a 20% testing dataset. A mean value of zero means that there was no difference between predicted and observed values, while a negative or positive mean indicates that predicted values were under or over predicted by linear models, respectively. A) Canopy structural complexity values were predicted by a model developed by stepwise regression with Landsat-derived metrics (80% training dataset). Predictive model coefficients can be found in Appendix 3: Table S3. B) Canopy structural complexity values were predicted by a model developed by simple linear regression with NDVI (80% training dataset). Linear model coefficients can be found in Appendix 3: Table S4. Error bars are the accelerated 95% confidence interval of each generated distribution are shown (Efron and Tibshirani, 1986).

complexity at the plot-level with linear models; but canopy water content was not significantly correlated with structural complexity. There were more significant linear relationships between Landsat-derived metrics and structural complexity metrics at the plot-level than at the site-level, and several of these relationships were significant at both levels for NDVI and EVI. The significant associations between canopy greenness and structural complexity metrics at both the site- and plot-level demonstrates that Landsat satellite imagery may contain additional structural information than previously realized. Our study suggests that Landsat-derived metrics could be used to infer structural characteristics of forest functional types at broad spatial extents.

Landsat-derived metrics of greenness were associated with metrics from all five categories of structural complexity, likely due to the importance of structural complexity as a driver of forest light acquisition and productivity (Hardiman et al., 2011; 2013; Atkins et al., 2018a). Linear relationships between greenness and structural complexity categories were consistent across Landsat-derived metrics of greenness with the exception of a weak positive, instead of a negative relationship, between TC greenness and porosity. Specifically, canopy greenness increased with greater canopy height, cover, density, and heterogeneity of vegetation distribution. This may be partially driven by efficient light interception in a more heterogeneous distribution of canopy vegetation (Atkins et al., 2018a) driving greater forest productivity and greenness (Niinemets, 2010). Furthermore, canopy height is positively correlated with species richness (Marks et al., 2016), which may lead to a heterogeneous canopy structure and niche partitioning of resource use, and ultimately increased ecosystem productivity (Fahey et al., 2016). Finally, canopy greenness decreased with greater porosity and foliar clumping. Greater foliar clumping is thought to increase ecosystem productivity, because it increases the amount of light reaching lower canopy levels and stimulates production of subcanopy vegetation (Gonsamo et al., 2017; Chen et al., 2012); thus, the observation of a decrease in greenness (i.e. lower productivity) with increased clumping was unexpected.

We found that canopy brightness was associated with several structural complexity measures, a result that is consistent with prior results showing 3D canopy structure influences the magnitude of reflectance. A brighter canopy was associated with greater vegetation area, canopy cover, porosity, variability in leaf height and lower foliar clumping. A canopy that exhibits more variation in leaf height, may be less reflective due to a greater surface complexity and more scattering of incident light (Ogunjemiyo et al., 2005; Atkins et al., 2018a). Tasseled cap brightness is typically used to distinguish soil from other land surface types, such as dense vegetation, because it is brighter; however tasseled cap greenness of vegetation has been shown to increase with brightness (Gemmell, 1995). Our sites were composed of heavily forested areas; thus, we would not expect a strong signature of brightness due to bare soil in our dataset (Gemmell, 1995). Our relationships between brightness and categories of structural complexity support this in our study, and the relationships largely support our use of brightness in this context. Albedo provides a measurement of canopy optical reflectance or whiteness (Ollinger et al., 2008) that is preferable to TC brightness. Therefore, future research endeavors could use a Landsat-derived albedo product, when it becomes widely available, to further explore the relationship between structural complexity and optical brightness of forest canopies.

Denser and more homogenous canopies were more uniformly saturated across Landsat pixels in our study, thereby reducing neighborhood variation in canopy greenness and brightness. Specifically, we found that the spatial variance of Landsat-derived metrics within plots (9-pixel neighborhood) was significantly related to structural complexity metrics. This could occur because Landsat-derived metrics can become saturated at higher levels of greenness or brightness and lead to low spatial variance within the saturation range of metric values; this is especially well documented for NDVI (Huete et al., 2002; Gitelson, 2004). If these Landsat-derived metrics are related to structural complexity, then positive or negative correlations of variance within a 9-pixel neighborhood and structural complexity metrics will occur. In

regression analyses, we might then expect to see outliers at high values of greenness. EVI may provide an alternative to reduce outliers from NDVI, because EVI is less sensitive to saturation in heavy vegetation (Huete et al., 2002).

Correlations between Landsat-derived indices and structural complexity were stronger and more abundant at the plot- rather than site-scale. One likely reason for this pattern was the lower statistical power at the site- than at the plot-level because our study used eight sites. However, several relationships between NDVI, EVI and structural complexity metrics were significant at both levels. Furthermore, these eight NEON sites originated from six ecoclimatic domains, and forest types from different domains may vary substantially in their forest structure, subsequently influencing the patterns observed in our study. For example, Ordway Swisher Biological Station (OSBS) is dominated by partially open-canopied savanna, with very different canopy structure than the closed-canopy forests that dominated other sites (e.g. Appendix 1: Fig. S1-5). The addition of sites from other ecoclimatic domains in future studies would increase the ecological applicability of our results across different forest types and beyond Eastern North America.

These results demonstrate that while Landsat vegetation metrics are most often used as a proxy for one dimensional structural measures summarizing the quantity of leaf area (Glenn et al., 2008; Fisher et al., 2018), these same metrics are also sensitive indicators of the arrangement of leaf area within canopies. In particular, NDVI robustly estimated six metrics of structural complexity from a validation dataset with linear models. Future efforts should expand this work to characterize additional forest types and ecoregions and explore the potential to create continent-scale estimates of canopy structural complexity by combining multiple remote sensing technologies and spatial scales.

5. Conclusions

Forest structure is a key driver of ecosystem processes and remote sensing can improve our understanding of canopy structural complexity. Our study suggests that Landsat-derived metrics contain information related not only to leaf area, but also of the arrangement of leaves within the canopy. Landsat-derived metrics of canopy greenness and brightness were correlated with several components of structural complexity from terrestrial LiDAR. The presence of these relationships at both site- and plot-levels between NDVI, EVI and structural complexity demonstrates the potential to use Landsat imagery to scale structural complexity estimates from plot to sub-continental scales. Although, correlations between Landsat-derived and structural complexity metrics were relatively strong, they were not 1:1, suggesting that accurately describing patterns of canopy structure at large spatial extents may require combining multiple remote sensing technologies. Thus, a next step should be to explore the potential development of large extent maps of structural complexity with Landsat and LiDAR technologies. Improved understanding of canopy structure can enhance our ability to predict ecosystem processes across wide spatial extents and ecoclimatic domains.

Acknowledgements

Funding was provided by NSF EF award #1550657 to C. Gough, #1550650 to R. Fahey, and #1550639 to B. Hardiman. E. LaRue was partially supported by NSF MSB-FRA award #1638702 to S. Fei and B. Hardiman. We thank two anonymous reviewers and the handing editor for providing feedback that improved the manuscript.

References

Atkins, J.W., Fahey, R.T., Hardiman, B.H., Gough, C.M., 2018a. Forest canopy structural complexity and light absorption relationships at the sub-continental scale. J. Geophys. Res. Biogeosci. 123, 1387–1405.

Atkins, J., Bohrer, G., Fahey, R., Hardiman, B., Morin, T., Stovall, A., Zimmerman, N., Gough, C., 2018b. Quantifying forestand canopy structural complexity metrics from terrestrial LiDAR data using the forestr R package. Methods Ecol. Evol. https://doi.org/10.1111/2041-210X.13061.

Baig, M.H.A., Zhang, L., Shuai, T., Tong, Q., 2014. Derivation of a tasselled cap transformation based on Landsat 8 satellite reflectance. Remote Sens. Lett. 5, 423–431.

Baldocchi, D.D., Harvey, P.C., 1995. Scaling carbon dioxide and water vapor exchange from leaf to canopy in a deciduous forest. II. Model testing and application. Plant Cell Environ. 18, 1157–1173.

Chen, J.M., Mo, G., Pisek, J., Liu, J., Deng, F., Ishizawa, M., Chan, D., 2012. Effects of foliage clumping on the estimation of global terrestrial gross primary productivity. Glob. Biogeochem. Cycles 26https://doi.org/10.1029/2010GB003996. GB1019.

Crist, E.P., Cicone, R.C., 1984. A physically-based transformation of thematic mapper data - the TM Tasseled Cap. Trans. Geosci. Remote Sens. 22, 256–263.

Dormann, C.F., Elith, J., Bacher, S., Buchmann, C., Carl, G., Carre, G., Garcia Marquez, J.R., Gruber, G., Lafourcade, B., Leitao, P.J., Munkemuller, T., McClean, C., Osborne, P.E., Reineking, B., Schroeder, B., Skidmore, A.K., Zurell, D.H., Lautenbach, S., 2013. Collinearity: a review of methods to deal with it and a simulation study evaluating their performance. Ecography 36, 27–46.

Efron, B.R., Tibshirani, 1986. Bootstrap methods for standard errors, confidence intervals, and other measures of statistical accuracy. Stat. Sci. 1, 54–75.

Fahey, R.T., Fotis, A.T., Woods, K.D., 2015. Quantifying canopy complexity and effects on productivity and resilience in late-successional hemlock-hardwood forests. Ecol. Appl. 25, 834–847.

Fahey, R.T., Stuart Haëntjens, E.J., Gough, C.M., De La Cruz, A., Stockton, E., Vogel, C.S., Curtis, P.S., 2016. Evaluating forest subcanopy response to moderate severity disturbance and contribution to ecosystem-level productivity and resilience. For. Ecol. Manage. 376, 135–147.

Fisher, R.A., Koven, C.D., Anderegg, W.R.L., Christoffersen, B.O., Dietze, M.C., Farrior, C., Holm, J.A., Hurtt, G., Knox, R.G., Lawrence, P.J., Lichststein, J.W., Longo, M., Matheny, A.M., Medvigy, D., Muller-Landau, H.C., Powell, T.L., Serbin, S.P., Sato, H., Shuman, J., Smith, B., Trugman, A.T., Viskari, T., Verbeeck, H., Weng, E., Xu, C., Xu, X., Zhang, T., Moorcroft, P., 2018. Spectral demographics in earth system models: a review of progress and priorities. Glob. Change Biol. 24, 35–54.

Freitas, S.R., Mello, M.C.S., Cruz, C.B.M., 2005. Relationships between forest structure and vegetation metrics in Atlantic rainforest. For. Ecol. Manage. 218, 353–362.

Funk, J.L., Lerdau, M.T., 2004. Photosynthesis in forest canopies. Forest Canopies 2, 335–358.

Gamon, J.A., Field, C.B., Goulden, M.L., Griffin, K.L., Hartley, A.E., Joel, G., Penuelas, J., Valentini, R., 1995. Relationships between NDVI, canopy structure, and photosynthesis in 3 Californian vegetation types. Ecol. Appl. 5, 28–41.

Gemmell, F.M., 1995. Effects of forest cover, terrain, and scale on timber volume estimation with thematic mapper data in a Rocky Mountain site. Remote Sens. Environ. 51, 291–305.

Gitelson, A.A., 2004. Wide dynamic range vegetation metric for remote quantification of biophysical characteristics of vegetation. J. Plant Physiol. 161, 165–173.

Glenn, E.P., Huete, A.R., Nagler, P.L., Nelson, S.G., 2008. Relationship between remotely-sensed vegetation metrics, canopy attributes and plant physiological processes: what vegetation metrics can and cannot tell us about the landscape. Sensors 8, 2136–2160.

Gonsamo, A., D'Odorico, P., Chen, J.M., Wu, C., Buchmann, N., 2017. Changes in vegetation phenology are not reflected in atmospheric CO2 and 13 C/12 C seasonality. Glob. Change Biol. 23, 4029–4044.

Hardiman, B.S., Bohrer, G., Gough, C.M., Vogel, C.S., Curtis, P.S., 2011. The role of canopy structural complexity in wood net primary production of a maturing northern deciduous forest. Ecology 92, 1818–1827.

Hardiman, B.S., Bohrer, G., Gough, C.M., Curtis, P.S., 2013a. Canopy structural changes following widespread mortality of canopy dominant trees. Forests 4, 537–552.

Hardiman, B.S., Gough, C.M., Halperin, A., Hofmeister, K.L., Nave, L.E., Bohrer, G., Curtis, P.S., 2013b. Maintaining high rates of carbon storage in old forests: a mechanism linking canopy structure to forest function. For. Ecol. Manage. 298, 111–119.

Huete, A., Didan, K., Miura, T., Rodriguez, E.P., Gao, X., Ferreira, L.G., 2002. Overview of the radiometric and biophysical performance of the MODIS vegetation metrics. Remote Sens. Environ. 83, 195–213.

Kao, R.H., Gibson, C.M., Gallery, R.E., Meier, C.L., Barnett, D.T., Docherty, K.M., Blevins, K.K., Travers, P.D., Azuaje, E., Springer, Y.P., Thibault, K.M., McKenzie, V.J., Keller, M., Alves, L.F., Hinckley, E.L.S., Parnell, J., Schimel, D., 2012. NEON terrestrial field observations: designing continental-scale, standardized sampling. Ecosphere 3.

Law, B.E., Kelliher, F.M., Baldocchi, D.D., Anthoni, P.M., Irvine, J., Moore, D., Van Tuyl, S., 2001. Spatial and temporal variation in respiration in a young ponderosa pine forest during a summer drought. Agric. For. Meteorol. 110, 27–43.

Marks, C.O., Muller-Landau, H.C., Tilman, D., 2016. Tree diversity, tree height and environmental harshness in eastern and western North America. Ecol. Lett. 19, 743–751.

Matasci, G., Hermosilla, T., Wulder, M.A., White, J.C., Coops, N.C., Hobart, G.W., Zald, S.J., 2018. Large-area mapping of Canadian boreal forest cover, height, biomass and other structural attributes using Landsat composites and lidar plots. Remote Sens. Environ. 209, 90–106.

Niinemets, U., 2010. A review of light interception in plant stands from leaf to canopy in different plant functional types and in species with varying shade tolerance. Ecol. Res. 25, 693–714.

Nychka, D., Nadkarni, N.M., 1990. Spatial Analysis of Points on Tree Structures: the Distribution of Epiphytes on Tropical Trees. University of North Carolina, Institute of Statistics Mimeograph Series No. 1971, Raleigh, NC, USA.

Ogunjemiyo, S., Parker, Geoffrey G., Roberts, D., 2005. Reflections in bumpy terrain: implications of canopy surface variations for the radiation balance of vegetation.

Geosci. Remote Sens. Lett. 2, 90–93.
Ollinger, S.V., Richardson, A.D., Martin, M.E., Hollinger, D.Y., Frolking, S.E., Reich, P.B., Plourde, L.C., Katul, G.G., Munger, J.W., Oren, R., Smith, M.L., Uaa, K.T.P., Bolstad, P.V., Cook, B.D., Day, M.C., Martin, T.A., Monson, R.K., Schmid, H.P., 2008. Canopy nitrogen, carbon assimilation, and albedo in temperate and boreal forests: functional relations and potential climate feedbacks. PNAS 105, 19336–19341.
Parker, G.G., Harding, D.J., Berger, M.L., 2004. A portable LiDAR system for rapid determination of forest canopy structure. J. Appl. Ecol. 41, 755–767.
Pitman, E.J.G., 1938. Significance tests which may be applied to samples from any populations. III. The analysis of variance test. Biometrika 29, 322–335.
Ren, Z.B., Zheng, H.F., He, X.Y., Zhang, D., Yu, X.Y., Shen, G.Q., 2015. Spatial estimation of urban forest structures with Landsat TM data and field measurements. Urban For. Urban Green. 14, 336–344.
Thomas, V., Noland, T., Treitz, P., McCaughey, J.H., 2011. Leaf area and clumping metrics for a boreal mixed-wood forest: lidar, hyperspectral, and Landsat models. Int. J. Remote Sens. 32, 8271–8297.
Tucker, C.J., 1979. Red and photographic infrared linear combinations for monitoring vegetation. Remote Sens. Environ. 8, 127–150. https://doi.org/10.1016/0034-4257(79.
Venables, W.N., Ripley, B.D., 2002. Modern Applied Statistics With S, fourth edition. Springer, New York ISBN 0-387-95457-0.
Zheng, G., Moskal, L.M., 2009. Retrieving leaf Area index (LAI) using remote sensing: theories, methods and sensor. Sensors 9, 2719–2745.